Cross sections for electron capture and excitation processes in collisions between the hydrogen-like $He^{+}(1s)$ and $B^{4+}(1s)$, $C^{5+}(1s)$, $N^{6+}(1s)$, $O^{7+}(1s)$ ions

V.K. Nikulin, N.A. Guschina

A.F. Ioffe Physical-Technical Institute, St. Petersburg, Russian Federation

Abstract

Cross sections for electron capture from the $He^{+}(1s)$ ion and for excitation of the $He^{+}(1s)$ ion in collisions with hydrogen-like $B^{4+}(1s)$, $C^{5+}(1s)$, $N^{6+}(1s)$, $O^{7+}(1s)$ ions have been obtained for the first time (collision energies E_c of the He^{+} ion are in the range 0.2 to 3 MeV). The calculations of cross sections were undertaken by the close-coupling equation method on the basis set of two-electron quasimolecular states.

Cross sections for single-electron capture into singlet and triplet 1snl ($2 \le n \le 5$) states of B^{3+}, C^{4+}, N^{5+}, O^{6+} ions differ insignificantly due to weak exchange interaction between ground and excited quasimolecular states. In $He^{+}(1s)$ - $C^{5+}(1s)$, $N^{6+}(1s)$, $O^{7+}(1s)$ collisions the main contribution at $E_c > 1$ MeV to total cross section for excitation of $He^{+}(1s)$ ion is due to electron excitation $1s \rightarrow 2p_0$. In $He^{+}(1s)$ - $B^{4+}(1s)$ collision significant contribution to the total cross section for excitation at $E_c < 1.0$ MeV is due to electron excitation $1s \rightarrow 3d_0$; at $E_c > 1.0$ MeV the process of electron excitation $1s \rightarrow 2p_{\pm 1}$ becomes the main one.

1. Introduction

In the central plasma region of controlled nuclear fusion devices, reactions occurring in collisions of He^{+} ions with hydrogen-like impurity ions B^{4+}, C^{5+}, N^{6+}, O^{7+} ($A^{(Za-1)+}$) within the MeV collision energy range are of great importance:

$$He^{+}(1s) + A^{(Za-1)+}(1s) \rightarrow \begin{cases} He^{2+} + A^{(Za-2)+}(1snl) \\ He^{+}(nl') + A^{(Za-1)+}(1s) \end{cases} \quad (1)$$

Direct experimental research of these collisions with strong Coulomb repulsion between ions is difficult, and these reactions have not yet been studied theoretically. We report calculations of total and partial cross sections for charge transfer and excitation in reactions (1), at collision energies of He^{+} ions ranging from 0.2 to 3 MeV.

The resulting data are necessary for modeling of alpha-particles behaviour in plasma and for spectroscopic diagnostics of high-temperature plasma. Emission from the excited impurity ions and He^{+} ions, formed after collision, is of interest for plasma core spectroscopic diagnostics.

2. Theoretical method

2.1. Two-electron quasimolecular states

Computation of cross sections for single-electron capture and excitation in reactions (1) were performed by means of the impact parameter approximation and solving the close-coupling equations on the basis set of two-electron quasimolecular states.

Two-electron quasimolecular states ϕ_j are calculated in the single configuration approximation constructed using the single-electron Screened Diatomic Molecular Orbitals (SDMO) ψ_j:

$$\phi_j(r_1, r_2, R) = \frac{1}{\sqrt{2(1+S_{0j}^2)}}(\psi_0(r_1;R)\ \psi_j(r_2;R) \pm \psi_0(r_2;R)) \equiv [\psi_0, \psi_j] \quad (2)$$

where R is the internuclear distance, r_1, r_2 are the coordinates of electrons, and ψ_0 is an orbital 1sσ or 1sσ' describing in the limit of separated atoms the 1s electron state of the ion $A^{(Za-1)+}$ or $A^{(Za-2)+}$. We use the classification of single-electron SDMOs by spherical quantum numbers (nlm) of united atom states. Signs "+" and "-" represent singlet and triplet two-electron states of quasimolecule; S_{0j} is the overlapping intergral of the SDMO ψ_0 and ψ_j, which are the solutions of the two-centre problem

$$(H_0(k)+V^j_{eff}(r_k;R))\ \psi_j(r_k)=\varepsilon_j(R)\ \psi_j(r_k),$$

$$H_0(k)=(-\frac{\nabla_k^2}{2}-\frac{Z_a}{r_{ak}}-\frac{Z_b}{r_{bk}}) \tag{3}$$

The effective potential V^j_{eff} is given in parametric form [2]:

$$V^j_{eff}(r_k;R)=\frac{1}{2}[\frac{a_1^j-b_1^j}{r_{ak}}+\frac{a_1^j+b_1^j}{r_{bk}}+\frac{\tilde{a}_1^j+Ra_0^j}{r_{ak}r_{bk}}+\frac{b_2^j(r_{ak}-r_{bk})^2}{Rr_{ak}r_{bk}}],$$

where r_{ak}, r_{bk} are distances from the k electron to the nuclei with charges Z_a and Z_b ($Z_b = Z_{He}$), respectively. The basic set of two-electron diabatic states $\phi_j = [\psi_0, \psi_j]$ used to calculate the reactions (1) is shown in Table I.

Table I. The Basic Set of Two-Electron Diabatic States $\phi_j(r_1,r_2;R)$ (SDMO 2pσ, 3dσ, 4fσ in ϕ_1 describe 1s electronic state of He^+ ion at $R \rightarrow \infty$)

$He^+ + B^{4+}$	$He^+ + C^{5+}$, N^{6+}	$He^+ + O^{7+}$	
the entrance channels $He^+(1s) + A^{(Za-1)}(1s)$			
ϕ_1 = [1sσ,2pσ]	ϕ_1 = [1sσ,3dσ]	ϕ_1 = [1sσ,4fσ]	
The charge-transfer channels $He^{2+} + A^{(Za-2)+}$(1snl)			
			(nl)
ϕ_2 = [1sσ',3dσ]	ϕ_2 = [1sσ',2pσ]	ϕ_2 = [1sσ',2pσ]	$2p_0$
ϕ_3 = [1sσ',4fσ]	ϕ_3 = [1sσ',4fσ]	ϕ_3 = [1sσ',3dσ]	$3d_0$
ϕ_5 = [1sσ',6hσ]	ϕ_4 = [1sσ',5gσ]	ϕ_4 = [1sσ',5gσ]	$4f_0$
ϕ_{10} = [1sσ',7iσ]	ϕ_6 = [1sσ',7iσ]	ϕ_5 = [1sσ',6hσ]	$5g_0$
ϕ_6 = [1sσ',2pπ]	-	-	$2p_{\pm1}$
ϕ_7 = [1sσ',3dπ]	ϕ_7 = [1sσ',3dπ]	ϕ_7 = [1sσ',3dπ]	$3d_{\pm1}$
ϕ_9 = [1sσ',5gπ]	ϕ_8 = [1sσ',4fπ]	ϕ_8 = [1sσ',4fπ]	$4f_{\pm1}$
-	ϕ_{10} = [1sσ',6hπ]	ϕ_9 = [1sσ',5gπ]	$5g_{\pm1}$
the excitation channels $He^+(n'l') + A^{(Za-1)+}(1s)$			
			(n'l')
ϕ_4 = [1sσ',5gσ]	ϕ_5 = [1sσ',6hσ]	ϕ_6 = [1sσ',7iσ]	$2p_0$
ϕ_8 = [1sσ',4fπ]	ϕ_9 = [1sσ',5gπ]	ϕ_{10} = [1sσ',6hπ]	$2p_{\pm1}$
ϕ_{11} = [1sσ',8kσ]	-	-	$3d_0$

Among single-electron orbitals ψ_j ($j \neq 0$) used to calculate reactions (1), there were SDMOs describing the 1s and $2p_{0,\pm1}$ electronic states of a He^+ ion and the $2p_0$, $3d_{0,\pm1}$, $4f_{0,\pm1}$, and $5g_{0,\pm1}$ electronic states of an $A^{(Za-2)+}$*(1snl)* ion in the limits of well separate nuclei. In the computation of $He^+(1s)$ - $B^{4+}(1s)$ collisions the excitation channel $3d_0$-state of He^+ ion, the nearest to the channel of single-electron capture into 1s5g-states of B^{3+} ion, was also taken into account. In this computation the single effective potential V^1_{eff} has been used, based on the parameter definition scheme described in Ref. [3]. To compute single-electron orbitals 1sσ and 1sσ′ with highly different energy values which describe the 1s-electon state in $A^{(Za-1)+}$ and $A^{(Za-2)+}$ ions at the limit of separated atoms, special effective potentials V^0_{eff} were used. Their parameter definition scheme is given in Ref. [4].

Energies of two-electron states $\phi_j(r_1,r_2;R)$

$$E_j(R)=<\phi_j(r_1,r_2;R)\,|\,H\,|\,\phi_j(r_1,r_2;R)> \tag{4}$$

have been calculated by means of the first order of perturbation theory [5], and are shown in Figs. 1-4.

A change from $Z_a = 5$ to $Z_a = 6$ and from $Z_a = 7$ to $Z_a = 8$ entails change of quasimolecular state $\phi_1(r_1,r_2;R)$, which describes at $R \rightarrow \infty$ the entrance channel in reactions (1). Atomic limits for two-electron states of $He^+(1s) + N^{6+}(1s)$ system, as shown in the Table I, were formulated on the basis of the following consideration: at the collision velocities under analysis, the probabilities of transitions between states [1sσ′,6hσ]-[1sσ′,7iσ] and [1sσ′,5gπ]-[1sσ′,6hπ] in the neighbourhood of their pseudocrossings at

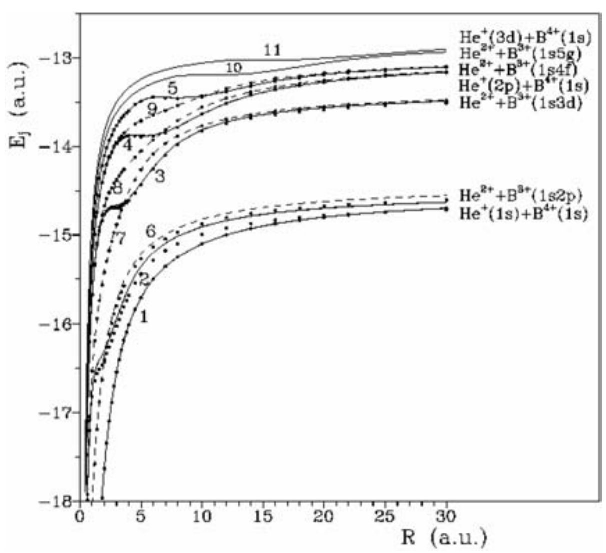

Figure 1. The energies $E_j(R)$ of two-electron singlet ($^1\Sigma_j$ - solid line, $^1\Pi_j$ - broken line) and triplet (•) diabatic states ϕ_j (j = 1 - 11) for the $He^+(1s) + B^{4+}(1s)$ system.
Entrance channel ϕ_1=[1sσ,2pσ] (1)
Charge-transfer channels:
ϕ_2=[1sσ′,3dσ] (2), ϕ_6=[1sσ′,2pπ] (6),
ϕ_3=[1sσ′,4fσ] (3), ϕ_7=[1sσ′,3dπ] (7),
ϕ_5=[1sσ′,6hσ] (5), ϕ_9=[1sσ′,5gπ] (9),
ϕ_{10}=[1sσ′,7iσ](10).
Single excitation channels:
ϕ_4=[1sσ′,5gσ] (4), ϕ_8=[1sσ′,4fπ] (8),
ϕ_{11}=[1sσ′,8kσ] (11).

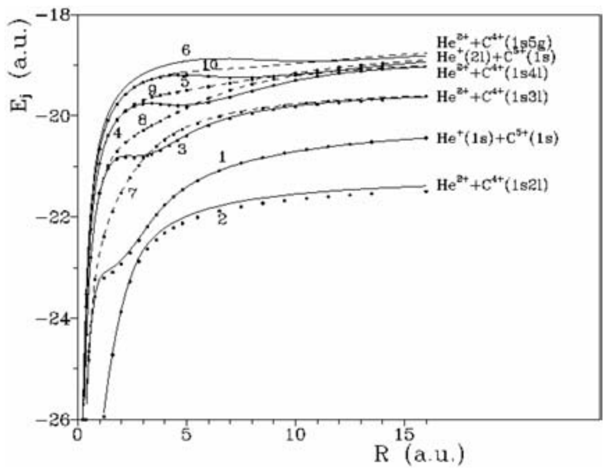

Figure 2. The energies E_j(R) of two-electron singlet ($^1\Sigma_j$ - solid line, $^1\Pi_j$ - broken line) and triplet (•) diabatic states ϕ_j (j = 1 - 10) for the $He^+(1s)$ + l$C^{5+}(1s)$ system.
Entrance channel ϕ_1=[1sσ,3dσ] (1).
Charge-transfer channels:
ϕ_2=[1sσ′,2pσ] (2),
ϕ_3=[1sσ′,4fσ] (3), ϕ_7=[1sσ′,3dπ] (7),
ϕ_4=[1sσ′,5gσ] (4), ϕ_8=[1sσ′,4fπ] (8),
ϕ_6=[1sσ′,7iσ] (6), ϕ_{10}=[1sσ′,6hπ] (10).
Single excitation channels:
ϕ_5=[1sσ′,6hσ] (5), ϕ_9=[1sσ′,5gπ] (9).

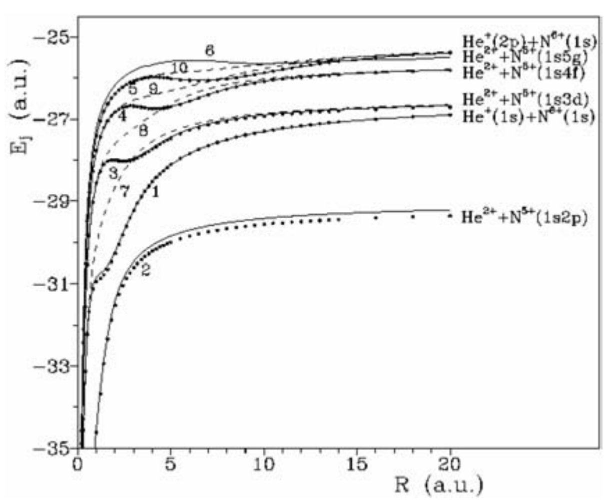

Figure 3. The energies E_j(R) of two-electron singlet ($^1\Sigma_j$ - solid line, $^1\Pi_j$ - broken line) and triplet ($^3\Sigma_j$ - •) diabatic states ϕ_j (j = 1 - 10) for the $He^+(1s)$ + $N^{6+}(1s)$ system.
a. Entrance channelϕ_1=[1sσ,3dσ] (1).
Charge-transfer channels:
ϕ_2=[1sσ′,2pσ] (2),
ϕ_3=[1sσ′,4fσ] (3), ϕ_7=[1sσ′,3dπ] (7),
ϕ_4=[1sσ′,5gσ] (4), ϕ_8=[1sσ′,4fπ] (8),
ϕ_5=[1sσ′,6hσ] (5), ϕ_9=[1sσ′,5gπ] (9).
c. Single excitation channels:
ϕ_6=[1sσ′,7iσ] (6), ϕ_{10}=[1sσ′,6hπ] (10).

R ~ 18 a.u. and R ~ 16 a.u. (see Fig. 3) equals 1; as a result the correlation diagram for the $He^+(1s)$ + $N^{6+}(1s)$ system is similar to the diagram for the $He^+(1s)$ + $C^{5+}(1s)$ system. Our calculations show that energies of the singlet and triplet states differ insignificantly in all considered systems because of the low exchange interaction between lower and excited electronic states.

2.2. Close-coupling equation method

Within the close-coupling equation method, the problem reduces to the determination of the electron wave function $\Psi(r_1,r_2,t)$, that satisfies the nonstationary Schrödinger equation

$$i\frac{\partial\Psi(r_1,r_2,t)}{\partial\ t} = H'(r_1,r_2,R(t))\Psi(r_1,r_2,t) \tag{5}$$

where H′ is the total electron Hamiltonian

$$H' = H + \frac{Z_a Z_b}{R(t)},\ H = \sum_{k=1,2} H_o(k) + \frac{1}{r_{12}} \tag{6}$$

$$\Psi(r_1,r_2,t) = \sum_{j=1}^{n} a_j(t)\phi_j(r_1,r_2,R)\exp(-i\int_0^t [E_j(R) + \frac{Z_a Z_b}{R}]dt') \tag{7}$$

and r_{12} is a distance between electrons.

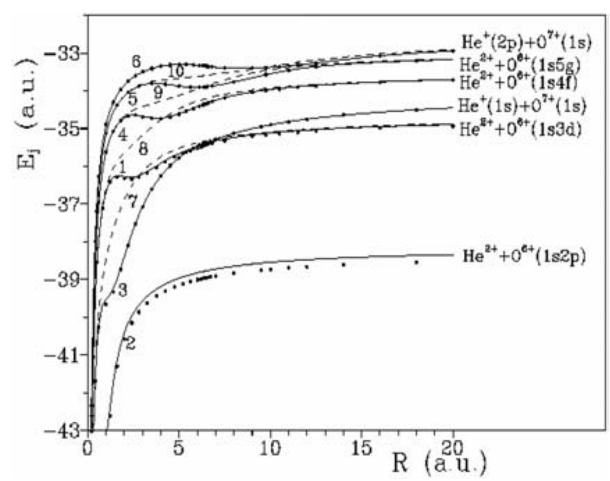

Figure 4. The energies E_j(R) of two-electron singlet ($^1\Sigma_j$ - solid line, $^1\Pi_j$ - broken line) and triplet ($^3\Sigma_j$ - •) diabatic states ϕ_j (j = 1 - 10) for the $He^+(1s)$ + $O^{7+}(1s)$ system.
Entrance channel ϕ_1=[1sσ,4fσ] (1).
Charge-transfer channels:
ϕ_2=[1sσ′,2pσ] (2),
ϕ_3=[1sσ′,3dσ] (3), ϕ_7=[1sσ′,3dπ] (7),
ϕ_4=[1sσ′,5gσ] (4), ϕ_8=[1sσ′,4fπ] (8),
ϕ_5=[1sσ′,6hσ] (5), ϕ_9=[1sσ′,5gπ] (9).
Single excitation channels:
ϕ_6=[1sσ′,7iσ] (6), ϕ_{10}=[1sσ′,6hπ] (10).

Wave function $\Psi(r_1,r_2,t)$ can be expanded into a series on the basis of a set of two-electron single configuration states:

If at $t \to -\infty$ ($R \to \infty$), the initial state of collision system $He^+(1s) + A^{(Za-1)+}(1s)$ is

$$\phi_1(r_1,r_2) = \lim_{t\to-\infty} \phi_1(r_1,r_2;R(t))$$

(with the energy $E_1(R=\infty)$), then

$$\Psi(r_1,r_2,t)|_{t\to-\infty} \to \phi_I(r_I,r_2)\exp(-iE_I(\infty)t). \tag{8}$$

Substitution of Eq. (7) into Eq. (5) and taking Eq. (8) into consideration gives a set of linear differential equations to determine a_j coefficients. For an orthogonal set of two-electron basis functions and the Coulomb trajectory of a nucleus motion, these equations can be re-arranged to give the following form [6]:

$$\frac{da_j(\tau)}{d\tau} = -\sum_{k\neq j} a_k(\tau)\{\frac{\tau}{R-\gamma}R_{jk} + \frac{\rho}{R(R-\gamma)}L_{jk}$$

$$+\frac{i}{\upsilon}\frac{R}{R-\gamma}H_{jk}\}\exp(-\frac{i}{\upsilon}\int_0^\tau (E_k - E_j)\frac{R}{R-\gamma}d\tau) \tag{9}$$

$$(R(\tau) = (\tau^2+\gamma^2+\rho^2)^{1/2}+\gamma;\ -\infty<\tau<\infty)$$

with these initial conditions

$$a_j(-\infty) = \delta_{1j}\exp(-i\nu_1), \tag{10}$$

where

$$\nu_1 = \exp(\frac{1}{\upsilon}\int_0^\infty [E_1(R) - E_1(\infty) + \frac{Z_aZ_b}{R}]\frac{R}{R-\gamma}d\tau\ ).$$

In Eq. (9) ρ is the impact parameter, and υ is the relative velocity of the nuclear motion, $\gamma = Z_aZ_b/(\mu\upsilon^2)$, μ - reduced mass; $R_{jk} = <\phi_j|d/dR|\phi_k>$, $L_{jk} = <\phi_j|iL_y|\phi_k>$ and $H_{jk} = <\phi_j|H|\phi_k>$ are matrix elements of dynamic (radial and rotational) and potential coupling between two-electron states (2).

The transition amplitude from the initial state $\phi_I(\mathbf{r}_1,\mathbf{r}_2)$ to the final state

$\phi_j(r_1,r_2) = \lim_{R\to\infty}\phi_j(r_1,r_2;R)$ for given impact parameter ρ and collision velocity υ is

$$b_j(\rho,\upsilon) = \lim_{t\to\infty} <\phi_j(r_1,r_2)|\ \Psi(r_1,r_2,t)> \exp(iE_j(\infty)t)$$

$$= a_j(\infty)\exp(-i\nu_j), \tag{11}$$

where

$$\nu_j = \frac{1}{\upsilon}\int_0^\infty [E_j(R) - E_j(\infty) + \frac{Z_aZ_b}{R}]\frac{R}{R-\gamma}d\tau. \tag{12}$$

In applying the quasi-molecular model to describe atomic collisions (i.e., in solving the close-coupling equations), the problem arises of electron momentum transfer in the course of charge exchange. Since the pioneering study [7], this problem has not yet been rigorously solved even when considering single-electron quasi-molecular processes. It was shown in Ref. [7] that, because of ignoring the electron momentum translation in the course of nucleus motion, the basis functions (electron states) in an expansion of Eq. (7) turn out to be coupled to each other for any nucleus positions. Hence, when the number n of the terms in the basis set is finite, the calculated results depend strongly on the set size. To eliminate the nonphysical coupling between the states, it was proposed in Ref. [7] to use basis molecular function of Eq. (2) multiplied by the translation factors in the form of plane waves in Eq. (7). Many different forms of the translation factors have been proposed for quasi-molecular and atomic bases, as well as for single-electron and two-electron colliding systems and for heteronuclear and homonuclear quasi-molecules.

In this study, an alternative approach proposed in Ref. [8] for single-electron quasi-molecules is used to take into account momentum transfer. A special coordinate system for electrons is used to calculate the matrix elements of the dynamic coupling of the states. It was shown in Ref. [8] that, if the coordinate origin in a heteronuclear quasi-molecule He^{2+}- H(1s) is set at the centroid of the charges on the inter-nuclear axis (equipotential point - a natural boundary that separates the electrons belonging to one nucleus from the electrons belonging to the other), the transition probabilities calculated as a function of the impact parameter and the total cross sections are close to those calculated after allowance for the translation factor in the form of a plane wave.

For two-electron quasi-molecules considered in this study, this approach was verified in our recent paper [9] by calculating the reverse processes to reactions (1). The results of our calculation were close to the results of quasi-molecular calculations performed in the low-energy range with allowance for the translation factor, and in the high-energy range using an atomic model. Moreover, the approach used in Ref. [9] provides the best agreement with the available experimental data over a wide energy range.

As matrix elements of dynamic and potential coupling between singlet and triplet states are equal to zero, the system of close-coupling Eqs. (10) for reactions (1) splits into two independent systems for singlet and triplet entrance channels.

Matrix elements of dynamic coupling d^s_{ij} and d^t_{ij} between singlet (s) and triplet (t) two-electron states are the same and can be expressed via the matrix elements of radial (R_{ij}) and rotational (L_{ij}) coupling between the single-electron SDMO ψ_i and ψ_j:

$$R_{ij} = <\psi_i\,|d/dR|\,\psi_j>,\quad if\quad m_i - m_j = 0; \tag{13}$$

$$L_{ij} = <\psi_i\,|iL_y|\,\psi_j>,\quad if\quad |m_i - m_j| = 1.$$

Expressions were obtained without allowance for a minor non-orthogonality between the ground ψ_o = (1sσ, 1sσ') and excited (ψ_i, ψ_j) states. The overlapping integral $S_{1s\sigma,1s\sigma'}$ was taken to be equal to one. For example, in the worst case of the $He^+(1s)$ – $B^{4+}(1s)$ collision system, the values of $S_{1s\sigma,2p\sigma}$ and $S_{1s\sigma',3d\sigma}$ are less than 2×10^{-2} and $S_{1s\sigma,1s\sigma'}$ = 0.996 ÷ 0.998 at all R.

Detailed information relative to matrix elements of dynamic and potential coupling for the collision systems under consideration is presented in our preliminary reports [10] and [11]. For example, only the following twelve most significant matrix elements of the dynamic coupling for the He^+– C^{5+} and He^+– N^{6+} collision systems were retained in the close-coupling equations written on the basis of ten two-electron states listed in Table I:

R_{12} = <3dσ|d/dR|2pσ>, R_{13} = <3dσ|d/dR|4fσ>,
R_{14} = <3dσ|d/dR|5gσ>, R_{15} = <3dσ|d/dR|6hσ>,
R_{34} = <4fσ|d/dR|5gσ>, R_{35} = <4fσ|d/dR|6hσ>,
R_{36} = <4fσ|d/dR|7iσ>, R_{45} = <5gσ|d/dR|6hσ>,
R^N_{46} = <5gσ|d/dR|7iσ>, R_{56} = <6hσ|d/dR|7iσ>,
R_{89} = <4fπ|d/dR|5gπ>, $R_{9,10}$ = <5gπ|d/dR|6hπ>.

The first three "transfer" matrix elements R_{12}, R_{13}, and R_{14}, between the entrance channel and charge-transfer channels (Table I) vanish asymptotically (Fig. 8, Ref. [10]). In calculations of the transfer matrix elements as discussed above, a special coordinate system for electron ("equipotential point frame" [8]) was used.

However, the "excitation" matrix element R_{15} calculated in the equipotential point frame possesses physically spurious asymptotic behaviour (Fig. 8, Ref. [10]) tending to a constant, and the attainment of convergence for the integrated solution of close-coupling equations becomes impossible. Therefore, the radial couplings between the entrance channel (ϕ_1) and the channels (ϕ_j) for the excitation into the $2p_0$ state of a He^+ ion that did not vanish at $R \to \infty$ were artificially cut off using an exponentially decaying function:

$$R'_{1j}(R) = R_{1j}(R_c)\exp[-\beta(R - R_c)] \qquad \text{for } R > R_c;$$
$$R'_{1j}(R) = R_{1j}(R) \qquad \text{for } R \le R_c,$$

where j = 4 for He^+– B^{4+} collision system, j = 5 for He^+– C^{5+} and He^+– N^{6+} collision systems and j = 6 for He^+– O^{7+} collision system (Table I). For all of the systems under study, the constants R_c and β were set to be about 7.0 and 0.3 a.u., respectively.

Only two out of the rest of the eight matrix elements R_{34} and R_{36} have spurious asymptotic behaviour (Fig. 11, Ref. [10]) . These eight matrix elements are responsible for the probability redistribution between charge-transfer and excitation channels. However, the results of integration of close-coupling equations are independent of whether matrix elements R_{34} and R_{36} are cut off or not.

All the computations of SDMO, two-electron states energies and matrix elements of dynamic and potential interaction between them are performed by using program package developed by the authors [12].

3. Results and discussions

For a given collision velocity υ, partial cross-sections of population of two-electron singlet and triplet states $\phi_j(r_1,r_2) = \lim_{R\to\infty} \phi_j(r_1,r_2;R)$ were calculated by means of the formula

$$\sigma_j(\upsilon) = 2\pi \int_0^\infty d\rho\, |b_j(\rho,\upsilon)|^2 \qquad (14)$$

where $b_j(\rho, \upsilon)$ are the transition amplitudes (12) from the initial state $\phi_1(r_1,r_2)$ to the final state $\phi_j(r_1,r_2)$ (the small non-orthogonality of the two-electron states ($<\phi_i|\phi_j> < 10^{-3}$) was not taken into account in the close-coupling equations (10)). The "TANGO" [13] program was used to integrate the close-coupling equations (kindly provided by Antoine Salin).

3.1. Cross sections for single-electron capture and excitation for $He^+(1s)$ - $B^{4+}(1s)$ collision

A calculation of partial cross sections $\sigma_j(\upsilon)$ (14) for $He^+(1s)$ ions colliding with $B^{4+}(1s)$ ions was carried out using the basic set of singlet two-electron states only. Total σ_{sec} and partial $\sigma_{sec}(n)$ cross sections for single-electron capture (sec) into singlet 1snl-states (n = 2 - 5) of B^{3+} ion were determined:

$$\sigma_{sec} = \sum_{n=2-3} \sigma_{sec}(n), \qquad (15)$$

where

$$\sigma_{sec}(2) = \sigma_2(2p_0) + \sigma_6(2p_{\pm1}),$$
$$\sigma_{sec}(3) = \sigma_3(3d_0) + \sigma_7(3d_{\pm1}),$$
$$\sigma_{sec}(4) = \sigma_5(4f_0) + \sigma_9(4f_{\pm1}),$$
$$\sigma_{sec}(5) = \sigma_{10}(5g_0)$$

total σ_{exc} and partial $\sigma_{exc}(2)$, $\sigma_{exc}(3)$ excitation (exc) cross sections of He^+ ion:

$$\sigma_{exc} = \sum_{n=2-5} \sigma_{exc}(n), \qquad (16)$$

where

$$\sigma_{exc}(2) = \sigma_{exc}(2p_0) + \sigma_{exc}(2p_{\pm1}) = \sigma_4(2p_0) + \sigma_7(2p_{\pm1}),$$
$$\sigma_{exc}(3) = \sigma_{exc}(3d_0) = \sigma_{11}(3d_0).$$

The basic set of 11 singlet two-electron quasimolecule states were used at projectile energies E_c of He^+ ion ranging from 0.2 to 2 MeV. Results are shown in Tables II and IIa, and in Figs. 5 and 6.

Contributions to the total single-electron capture and excitation cross sections of the single-electron capture processes and excitation into triplet quasimolecular states are discussed in the following section.

3.2. Cross sections for single-electron capture and excitation for $He^+(1s)$ - $C^{5+}(1s)$ collision

Solutions of the close-coupling equation system for the $He^+ + C^{5+}$ quasimolecule on the basic set of 10 two-electron quasimolecilar states were determined for both the singlet and triplet entrance channel. Total σ_{sec} and partial $\sigma_{sec}(n)$ cross sections for single-electron capture into singlet and triplet 1snl-states with n = 2 - 5 of C^{4+} ion were calculated by the formula:

$$\sigma_{sec} = \sum_{n=2-5} \sigma_{sec}(n), \tag{17}$$

where

$\sigma_{sec}(2) = \sigma_2(2p_0)$, $\sigma_{sec}(3) = \sigma_3(3d_0) + \sigma_7(3d_{\pm 1})$, $\sigma_{sec}(4) = \sigma_4(4f_0) + \sigma_8(4f_{\pm 1})$, $\sigma_{sec}(5) = \sigma_6(5g_0) + \sigma_{10}(5g_{\pm 1})$;

total σ_{exc} and partial $\sigma_{exc}(2p_{0,\pm 1})$ excitation cross sections of He^+ ion were calculated as follows:

$$\sigma_{exc} = \sigma_{exc}(2p_0) + \sigma_{exc}(2p_{\pm 1}),$$

where

$$\sigma_{exc}(2p_0) = \sigma_5(2p_0), \quad \sigma_{exc}(2p_{\pm 1}) = \sigma_9(2p_{\pm 1}).$$

The calculations show that partial cross sections for the single-electron capture and excitation, determined on the basic set of singlet and triplet $He^+ + C^{5+}$ quasimolecule states, exhibited insignificant differences (for comparsion, total cross sections for charge transfer and excitation into singlet and triplet quasimolecular states are shown in Figs. 7 and 8). These observations occur because the energies of the singlet and triplet states only differ by a small amount due to their low exchange interaction, and the matrix elements of the dynamic interaction between singlet (d^s_{ij}) and triplet (d^{tr}_{ij}) states are equal. The results of the calculation of the partial (for singlet entrance channel) and total (for singlet and triplet entrance channels) cross sections for charge transfer and excitation processes are shown in Tables III and IIIa, and in Figs. 7 and 8.

Table II. The Partial $\sigma_{sec}(n)$ and Total σ_{sec} Cross Sections for Single-Electron Capture of Singlet 1snl-States of B^{3+} in $He^+(1s) + B^{4+}(1s)$ Collisions

E_C (MeV)	$\sigma_{sec}(n = 2)$ (10^{-16} cm^2)	$\sigma_{sec}(n = 3)$ (10^{-16} cm^2)	$\sigma_{sec}(n = 4)$ (10^{-16} cm^2)	$\sigma_{sec}(n = 5)$ (10^{-16} cm^2)	σ_{sec} (10^{-16} cm^2)
0.20	5.65	1.01	0.38	0.05	7.08
0.25	6.02	1.39	1.47	0.07	8.86
0.30	5.95	1.69	1.90	0.13	9.67
0.35	4.49	2.99	2.07	0.45	10.00
0.40	4.18	3.58	2.38	0.90	11.04
0.45	3.75	4.27	2.92	1.66	12.60
0.50	3.76	4.81	3.27	2.53	14.37
0.60	4.36	5.59	4.44	4.47	18.87
0.70	4.76	6.19	5.32	6.55	22.81
0.80	5.29	6.56	5.85	8.24	25.94
1.00	6.23	7.06	6.54	10.67	30.51
1.20	6.14	7.57	6.87	11.79	32.37
1.40	5.70	8.03	7.68	11.97	33.38
1.60	5.46	8.25	8.72	1.095	33.38
1.80	5.28	8.52	10.48	9.98	34.26
2.00	5.24	8.73	12.53	8.83	35.33

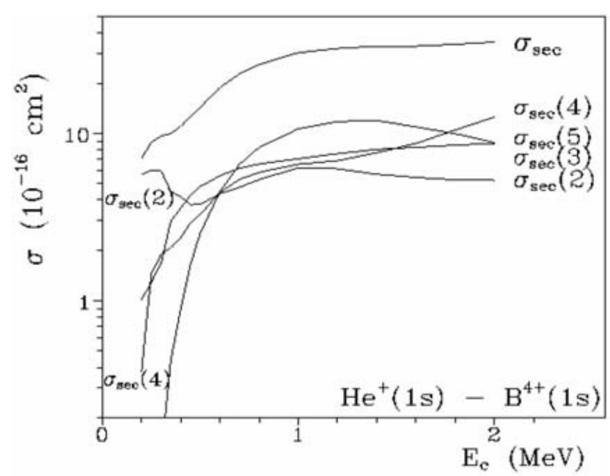

Figure 5. The total σ_{sec} and partial $\sigma_{sec}(n)$ cross sections for the single-electron capture in $He^+(1s) + B^{4+}(1s)$ collisions: $\sigma_{sec} = \sum_{n=2-5} \sigma_{sec}(n)$; $\sigma_{sec}(2) = \sigma_2(2p_0)+\sigma_6(2p_{\pm 1})$, $\sigma_{sec}(3) = \sigma_3(3d_0)+\sigma_7(3d_{\pm 1})$, $\sigma_{sec}(4) = \sigma_4(4f_0)+\sigma_9(4f_{\pm 1})$, $\sigma_{sec}(5) = \sigma_{10}(5g_{\pm 1})$.

Table IIa. The Partial $\sigma_{exc}(2p_l)$, $\sigma_{exc}(3d_0)$ and Total σ_{exc} Cross Sections for $He^+(1s)$ Ion Excitation in $He^+(1s) + B^{4+}(1s)$ Collisions for the Singlet Entrance Channel

E_C (MeV)	$\sigma_{exc}(2p_0)$ (10^{-16} cm^2)	$\sigma_{exc}(2p_{\pm1})$ (10^{-16} cm^2)	$\sigma_{exc}(3d_0)$ (10^{-16} cm^2)	σ_{exc} (10^{-16} cm^2)
0.20	0.09	0.09	0.10	0.28
0.25	0.11	0.13	0.14	0.38
0.30	0.10	0.26	0.29	0.65
0.35	0.52	0.63	0.45	1.60
0.40	0.69	1.04	0.90	2.62
0.45	0.86	1.62	1.90	4.38
0.50	1.07	2.35	2.79	6.21
0.60	1.31	4.05	4.86	10.22
0.70	1.77	5.84	7.60	15.22
0.80	2.37	7.45	9.75	19.57
1.00	3.67	9.79	11.35	24.81
1.20	4.58	11.02	11.62	27.22
1.40	5.19	11.42	11.23	27.83
1.60	6.21	11.24	11.06	28.52
1.80	7.30	10.80	10.55	28.66
2.00	8.60	10.22	10.14	28.95

Total cross sections for single-electron capture (Σ_{sec}) and excitation (Σ_{exc}) in the $He^+(1s)$ - $C^{5+}(1s)$ collision are equal:

$$\Sigma_{sec} = 0.25\ \sigma^{s}_{sec} + 0.75\ \sigma^{tr}_{sec} \text{ and } \Sigma_{exc}(2p_l) = 0.25\ \sigma^{s}_{exc} + 0.75\ \sigma^{tr}_{exc}, \tag{18}$$

where σ^s_{sec}, σ^s_{exc} and σ^{tr}_{sec}, σ^{tr}_{exc} are the total cross sections for charge transfer and excitation, calculated for the singlet and triplet two-electron quasimolecule states, respectively.

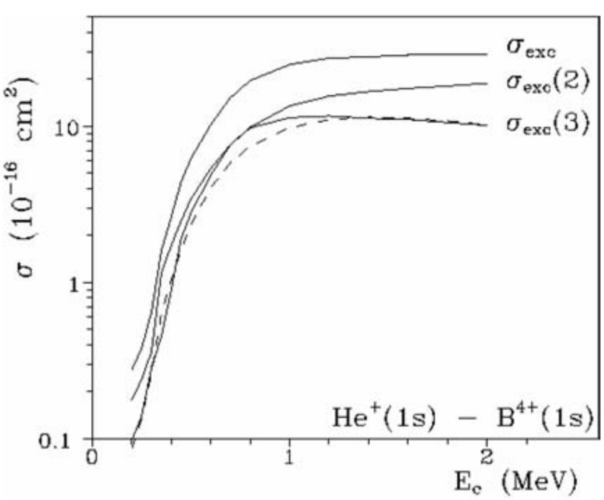

Figure 6. The total σ_{exc} and partial $\sigma_{exc}(n)$ cross sections for the $He^+(1s)$ ion excitation in $He^+(1s) + B^{4+}(1s)$ collisions: $\sigma_{exc} = \sigma_{exc}(2)+\sigma_{exc}(3)$; $\sigma_{exc}(2) = \sigma_{exc}(2p_0)+\sigma_{exc}(2p_{\pm1}) = \sigma_4+\sigma_{10}$, $\sigma_{exc}(3) = \sigma_{exc}(3d_0) = \sigma_{11}$ (broken line - partial $\sigma_{exc}(2p_{\pm1})$ cross section).

3.3. Cross sections for single-electron capture and excitation for $He^+(1s)$ - $N^{6+}(1s)$, $O^{7+}(1s)$ collisions

Taking into account the results of detailed research on the $He^+(1s)$ - $C^{5+}(1s)$ collision process, the calculations of single-electron capture and excitation cross sections for $He^+(1s)$ ions colliding with $B^{4+}(1s)$, $N^{6+}(1s)$ and $O^{7+}(1s)$ ions were performed using the basic set of singlet two-electron states only. Cross sections calculated on the basis of these given conditions describe the statistically weighted total

Table III. The Partial $\sigma_{sec}(n)$ and Total σ_{sec} Cross Sections for the Single-Electron Capture of Singlet 1snl-States of C^{4+} in $He^+(1s) + C^{5+}(1s)$ Collisions (σ_{sec}^{tr} – Total Cross Section for the Single-Electron Capture Triplet 1snl-States of C^{4+} Ions)

E_C (MeV)	$\sigma_{sec}(n = 2)$ (10^{-16} cm^2)	$\sigma_{sec}(n = 3)$ (10^{-16} cm^2)	$\sigma_{sec}(n = 4)$ (10^{-16} cm^2)	$\sigma_{sec}(n = 5)$ (10^{-16} cm^2)	$\sigma_{sec}(\sigma^{tr}_{sec})$ (10^{-16} cm^2)
0.200	2.21	3.64	1.35	0.70	7.90 (8.48)
0.267	2.05	6.55	2.27	1.65	12.52
0.400	1.76	7.80	2.46	3.23	15.24
0.533	1.07	7.10	3.30	4.84	16.31
0.667	0.53	6.49	4.35	6.40	17.77
0.800	0.42	6.04	5.70	7.65	19.81
0.933	0.40	5.88	7.42	8.27	21.96
1.067	0.43	5.78	8.84	8.72	23.76
1.333	0.67	5.71	11.07	8.72	26.16
1.600	1.04	5.64	12.20	8.67	27.55 (27.91)
2.000	1.57	5.84	12.58	7.56	27.56 (29.05)
2.333	1.74	6.05	12.58	7.35	27.73
2.667	1.76	6.32	12.52	7.25	27.84
3.000	1.73	6.53	12.47	7.25	27.99

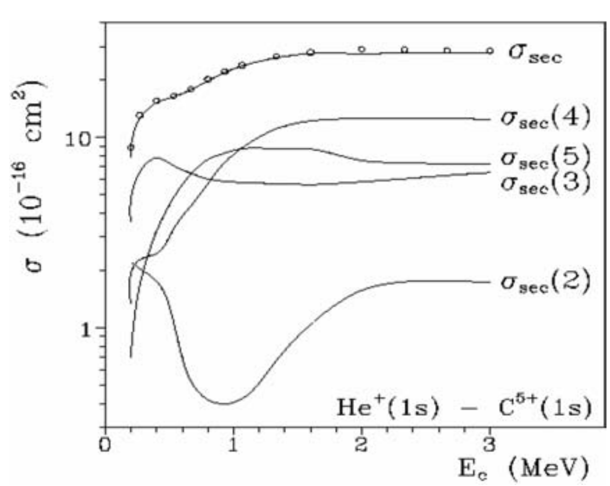

Figure 7. The total σ_{sec} and partial $\sigma_{sec}(n)$ cross sections for the single-electron capture in $He^+(1s) + C^{5+}(1s)$ collisions: $\sigma_{sec} = \sum_{n=2-5} \sigma_{sec}(n)$; $\sigma_{sec}(2) = \sigma_2(2p_0)$, $\sigma_{sec}(3) = \sigma_3(3d_0)+\sigma_7(3d_{\pm1})$, $\sigma_{sec}(4) = \sigma_4(4f_0)+\sigma_8(4f_{\pm1})$, $\sigma_{sec}(5) = \sigma_6(5g_0)+\sigma_{10}(5g_{\pm1})$

cross sections (20) of charge transfer and excitation for the $He^{+}(1s)$ - $B^{4+}(1s)$, $N^{6+}(1s)$, $O^{6+}(1s)$ collisions with a high degree of accuracy.

Table IIIa. The Partial $\sigma_{exc}(2p_l)$ and Total σ_{exc} Cross Sections for the $He^{+}(1s)$ Ion Excitation in $He^{+}(1s)$ + $C^{5+}(1s)$ Collisions for the Singlet Entrance Channel ($\sigma_{exc}{}^{tr}$ – Total Excitation Cross Section for the Triplet Entrance Channel)

E_C (MeV)	$\sigma_{exc}(2p_0)$ (10^{-16} cm^2)	$\sigma_{sec}(2p_{\pm1})$ (10^{-16} cm^2)	$\sigma_{exc}(\sigma^{tr}{}_{exc})$ (10^{-16} cm^2)
0.200	0.07	0.14	0.21 (0.34)
0.267	0.13	0.36	0.49 (0.59)
0.400	1.35	1.14	2.49 (2.73)
0.533	3.38	3.04	6.42 (6.79)
0.667	5.90	5.70	11.60 (11.95)
0.800	8.65	8.53	17.17 (17.58)
0.933	11.46	11.06	22.52 (22.55)
1.067	13.69	13.14	26.83 (26.71)
1.333	17.17	15.87	33.04 (32.61)
1.600	19.30	17.17	36.47 (36.10)
2.000	21.44	17.50	38.94 (38.44)
2.333	22.45	17.08	39.53 (39.18)
2.667	23.12	16.39	39.51 (39.26)
3.000	23.52	15.62	39.14 (38.96)

Total and partial cross sections for single-electron capture and excitation of collisions between $He^{+}(1s)$ ions and $N^{6+}(1s)$ ions were calculated by means of Eqs. (17) and (18). The data are shown in Tables IV and IVa, and in Figs. 9 and 10.

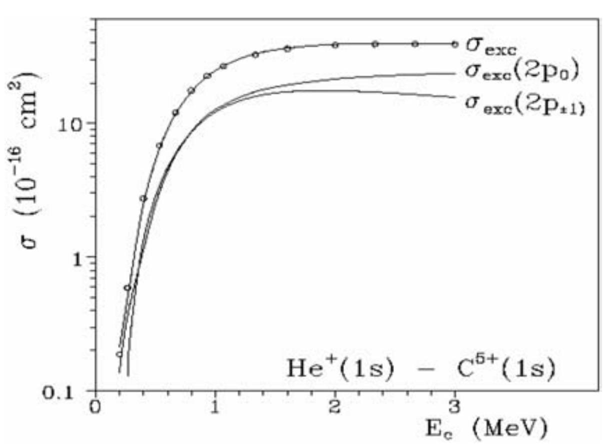

Figure 8. The total σ_{exc} and partial $\sigma_{exc}(2p_l)$ cross sections for $1s \rightarrow 2p_l$ electron excitation of the $He^{+}(1s)$ ion in $He^{+}(1s)$ + $C^{5+}(1s)$ collisions: $\sigma_{exc} = \sigma_{exc}(2p_0)+ \sigma_{exc}(2p_{\pm1})$; $\sigma_{exc}(2p_0) = \sigma_5$, $\sigma_{exc}(2p_{\pm1}) = \sigma_9$ (total excitation cross section $\sigma_{exc}{}^{tr}$ calculated on the basis of the triplet quasimolecular state)

When the cross sections for single-electron capture and excitation of collisions between $He^{+}(1s)$ ions and $O^{7+}(1s)$ ions were calculated, Eqs. (18) and (19) for the partial cross sections $\sigma_{sec}(5)$ and $\sigma_{exc}(2p_l)$ were changed in the following way:

$\sigma_{sec}(5) = \sigma_5(5g_0)+\sigma_9(5g_{\pm1})$ and $\sigma_{exc}(2p_0) = \sigma_6(2p_0)$, $\sigma_{exc}(2p_{\pm1}) = \sigma_{10}(2p_{\pm1})$.

The data are shown in Tables V and Va, and in Figs. 11 and 12.

Table IV. The Partial $\sigma_{sec}(n)$ and Total σ_{sec} Cross Sections for the Single-Electron Capture of Singlet 1snl-States of N^{5+} in $He^{+}(1s)$ + $N^{6+}(1s)$ Collisions

E_C (MeV)	$\sigma_{sec}(n = 2)$ (10^{-16} cm^2)	$\sigma_{sec}(n = 3)$ (10^{-16} cm^2)	$\sigma_{sec}(n = 4)$ (10^{-16} cm^2)	$\sigma_{sec}(n = 5)$ (10^{-16} cm^2)	σ_{sec} (10^{-16} cm^2)
0.20	1.15	5.73	0.66	0.47	8.01
0.40	0.45	7.02	5.66	2.34	15.48
0.60	0.17	4.72	11.71	6.24	22.84
0.80	0.11	3.61	13.25	9.51	26.48
1.00	0.08	3.10	12.52	11.58	27.28
1.20	0.07	2.78	11.29	12.54	26.68
1.50	0.07	2.49	9.78	12.63	24.96
1,70	0.08	2.37	8.96	12.13	23.54
2.00	0.10	2.35	8.44	11.46	22.35
2.50	0.13	2.48	7.64	10.50	20.74
3.00	0.16	2.98	7.10	9.68	19.92

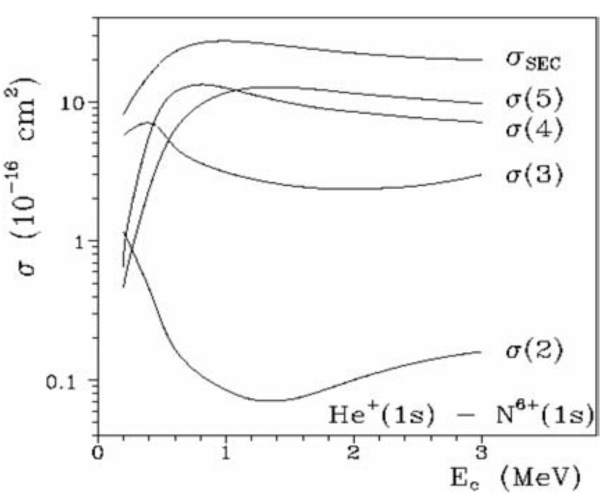

Figure 9. The total σ_{sec} and partial $\sigma_{sec}(n)$ cross section for the single-electron capture in $He^{+}(1s)$ + $N^{6+}(1s)$ collisions: $\sigma_{sec} = \sum_{n=2-5} \sigma_{sec}(n)$; $\sigma_{sec}(2) = \sigma_2(2p_0)$, $\sigma_{sec}(3) = \sigma_3(3d_0) + \sigma_7(3d_{\pm1})$, $\sigma_{sec}(4) = \sigma_4(4f_0) + \sigma_8(4f_{\pm1})$, $\sigma_{sec}(5) = \sigma_6(5g_0) + \sigma_{10}(5g_{\pm1})$.

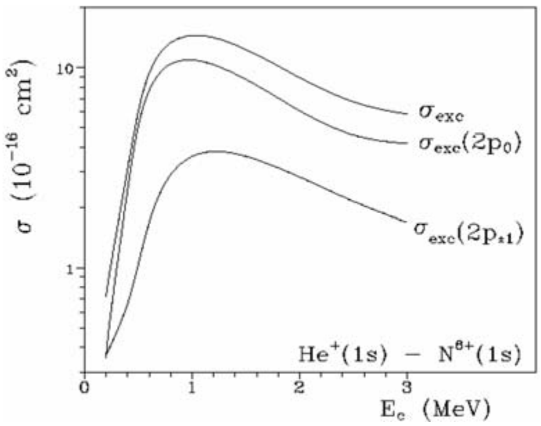

Figure 10. The total σ_{exc} and partial $\sigma_{exc}(2p_l)$ cross sections for the $1s \to 2p_l$ electron excitation of $He^+(1s)$ ion in $He^+(1s) + N^{6+}(1s)$ collisions: $\sigma_{exc} = \sigma_{exc}(2p_0) + \sigma_{exc}(2p_{\pm1})$; $\sigma_{exc}(2p_0) = \sigma_5(2p_0)$, $\sigma_{exc}(2p_{\pm1}) = \sigma_9(2p_{\pm1})$.

Table IVa. The Partial $\sigma_{exc}(2_l)$ and Total σ_{exc} Cross Sections of the $He^+(1s)$ Ion Excitation in $He^+(1s) + N^{6+}(1s)$ Collisions for the Singlet Channel

E_C (MeV)	$\sigma_{exc}(2p_0)$ (10^{-16} cm^2)	$\sigma_{exc}(2p_{\pm1})$ (10^{-16} cm^2)	σ_{exc} (10^{-16} cm^2)
0.20	0.36	0.36	0.72
0.40	2.45	0.66	3.11
0.60	7.66	1.68	9.34
0.80	10.44	2.90	13.34
1.00	10.93	3.60	14.52
1.20	10.35	3.80	14.16
1.50	8.75	3.60	12.35
1.70	7.32	3.23	10.56
2.00	6.09	2.84	8.93
2.50	4.61	2.14	6.75
3.00	4.18	1.69	5.87

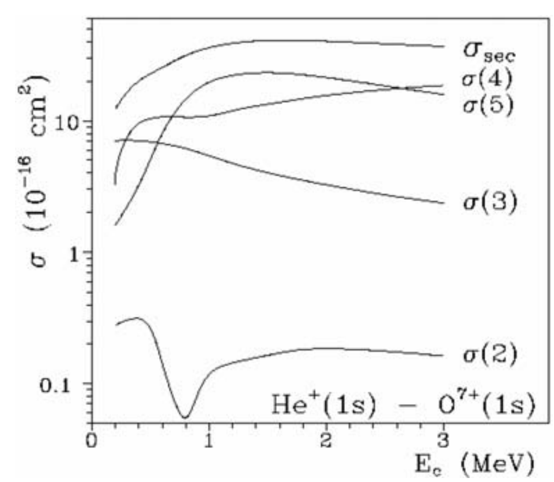

Figure 11. The total σ_{sec} and partial $\sigma_{sec}(n)$ cross sections for the single-electron capture in $He^+(1s) + O^{7+}(1s)$ collisions: $\sigma_{sec} = \sum_{n=2-5} \sigma_{sec}(n)$; $\sigma_{sec}(2) = \sigma_2(2p_0)$, $\sigma_{sec}(3) = \sigma_3(3d_0)+\sigma_7(3d_{\pm1})$, $\sigma_{sec}(4) = \sigma_4(4f_0)+\sigma_8(4f_{\pm1})$, $\sigma_{sec}(5) = \sigma_5(5g_0)+\sigma_9(5g_{\pm1})$.

Table V. The Partial $\sigma_{sec}(n)$ and Total σ_{sec} Cross Sections for the Single-Electron Capture of Singlet 1snl-States of O^{6+} in $He^+(1s) + O^{7+}(1s)$ Collisions

E_C (MeV)	$\sigma_{sec}(n = 2)$ (10^{-16} cm^2)	$\sigma_{sec}(n = 3)$ (10^{-16} cm^2)	$\sigma_{sec}(n = 4)$ (10^{-16} cm^2)	$\sigma_{sec}(n = 5)$ (10^{-16} cm^2)	σ_{sec} (10^{-16} cm^2)
0.20	0.28	7.05	3.29	1.59	12.22
0.40	0.31	7.04	9.56	3.22	20.13
0.60	0.14	6.70	10.69	7.98	25.51
0.80	0..05	6.15	10.65	14.64	31.49
1.00	0.11	5.40	10.89	19.73	36.14
1.25	0.15	4.59	12.23	22.57	39.53
1.50	0.16	4.02	13.38	23.28	40.85
1.75	0.18	3.59	14.54	22.65	40.95
2.00	0.18	3.25	15.59	21.39	40.42
2.50	0.18	2.72	17.32	18.46	38.68
3.00	0.16	2.36	18.60	15.86	36.98

Table Va. The Partial $\sigma_{exc}(2p_l)$ and Total σ_{exc} Cross Sections for the $He^+(1s)$ Ion Excitation in $He^+(1s) + O^{7+}(1s)$ Collisions for the Singlet Entrance Channel

E_C (MeV)	$\sigma_{exc}(2p_0)$ (10^{-16} cm^2)	$\sigma_{sec}(2p_{\pm1})$ (10^{-16} cm^2)	σ_{exc} (10^{-16} cm^2)
0.20	0.92	0.29	1.21
0.40	1.38	1.23	2.60
0.60	3.93	3.28	7.21
0.80	6.54	4.67	11.21
1.00	8.72	5.35	14.07
1.25	11.10	5.59	16.68
1.50	12.77	5.56	18.33
1.75	14.32	5.45	19.77
2.00	15.87	5.33	21.20
2.50	18.98	5.12	24.10
3.00	21.84	4.99	26.83

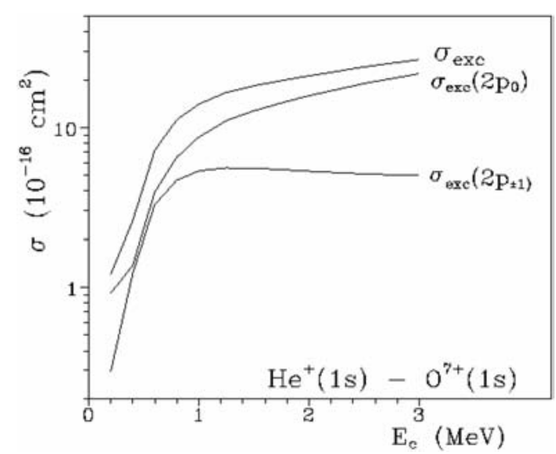

Figure 12. The total σ_{exc} and partial $\sigma_{exc}(2p_l)$ cross sections for the $1s \to 2p_l$ electron excitation of the $He^+(1s)$ ion in $He^+(1s) + O^{7+}(1s)$ collisions: $\sigma_{exc} = \sigma_{exc}(2p_0)+ \sigma_{exc}(2p_{\pm1})$; $\sigma_{exc}(2p_0) = \sigma_6(2p_0)$, $\sigma_{exc}(2p_{\pm1}) = \sigma_{10}(2p_{\pm1})$.

4. Conclusion

New data have been obtained on the total and partial cross sections for single-electron capture and excitation of the projectile in collision between hydrogen-like $He^+(1s)$ and $B^{4+}(1s)$, $C^{5+}(1s)$, $N^{6+}(1s)$, $O^{7+}(1s)$ ions over a range of collision energies E_c from 0.2 to 3.0 MeV. The maximum value of the total cross section for single-electron capture (40.9×10^{-16} cm^2) was obtained in the $He^+(1s)$ - $O^{7+}(1s)$ collision at E_c = 1.75 MeV. The maximum value of the excitation total cross section of the He^+ ion (39.5×10^{16} cm^2) was obtained in a collision between $He^+(1s)$ and $C^{5+}(1s)$ ions at E_c = 2.33 MeV. In the $He^+(1s) + B^{4+}(1s)$, $N^{6+}(1s)$, $O^{7+}(1s)$ collisions, cross sections for single-electron capture are larger than the cross section for excitation over the whole range of considered collision energies, and for the $He^+(1s) + C^{5+}(1s)$ collision is only larger when E_c < 0.9 MeV. At low collision energies in all of the systems considered with the exception of $He^+(1s) + B^{4+}(1s)$, the main single-electron capture occurs in the 1s3l-states of $A^{(Z_A-2)+}$ ions. As E_c increases (a) in $He^+(1s) + C^{5+}(1s)$ collisions, the main single-electron capture occurs in the 1s5l- and then the 1s4l-states of C^{4+} ion; (b) in $He^+(1s) + N^{6+}(1s)$ collisions, single-electron capture occurs in the 1s4l- and then the 1s5l-states of N^{5+} ions; (c) in $He^+(1s) + O^{7+}(1s)$ collisions, most of single-electron capture occurs in the 1s4l- and then the 1s5l-states followed by the 1s4l-states of the O^{6+} ion. At low collision energies E_c, in the $He^+(1s) + B^{4+}(1s)$ collision, the main single-electron capture involves the 1s2l-state of B^{3+} ion; whereas for all other collisions, the partial cross section for single-electron capture in the 1s2p-state of the $A^{(Z_A-2)+}$ ion is small over the whole range of collision energies considered:

$\sigma^C_{sec}(2) < 2.0\ 10^{-16}$ cm^2, $\sigma^N_{sec}(2) < 1.\ 10^{-16}$ cm^2 and $\sigma^0_{sec}(2) < 0.3\ 10^{-16}$ cm^2.

For the $He^+(1s) + B^{4+}(1s)$ collision, capture in the 1s3l- followed by the 1s5l-states of B^{3+} ion are the most significant E_c increases. We list below the E_c intervals (in MeV) for every system in which the maximun values of the partial single-electron capture cross sections in n-states of $A^{(Z_A-2)+}(1snl)$ ions were obtained (maximum values for the partial cross sections $\sigma(n)$ (in 10^{-16} cm^2) over each interval are listed in parentheses):

	n = 2	n = 3
$B^{3+}(1snl)$	$E_c < 0.4$ (6.00)	-
$C^{4+}(1snl)$	-	$E_c < 0.7$ (7.8)
$N^{5+}(1snl)$	-	$E_c < 0.4$ (7.0)
$O^{6+}(1snl)$	-	$E_c < 0.4$ (7.1)

n = 4	n = 5
$0.4 < E_c < 0.7$ (6.2)	$E_c > 0.7$ (12.6)
$E_c > 1.0$ (12.6)	$0.7 < E_c < 1.0$ (8.7)
$0.4 < E_c < 1.1$ (13.3)	$E_c > 1.1$ (12.6)
$0.4 < E_c < 0.70$ (10.7)	$0.7 < E_c < 2.6$ (23.3)
$E_c > 2.6$ (20.3)	

The excitation of the He^+ ion in $He^+(1s) + C^{5+}(1s)$, $N^{6+}(1s)$, $O^{7+}(1s)$ collisions occurs mainly in the $2p_0$-state. A significant contribution to the total cross section in the $He^+(1s)$ - $B^{4+}(1s)$ collision is made by excitation in the $3d_0$-state of the He^+ ion.

This work has been supported by the IAEA (Research Contract N 100088/Regular Budget Fund).

References

[1] TAWARA, H., "Roles of Atomic and Molecular Processes in Fusion Plasma Researches", NIFS- DATA-25, May 1995, Nagoya, Japan.

[2] NIKULIN, V.K., GUSCHINA, N.A., J. Phys B: Atom. Mol. Phys. **11** (1978) 3553.

[3] NIKULIN, V.K., GUSCHINA, N.A., Tech. Phys. **44** (1999) 12 (translated from Russian).

[4] NIKULIN, V.K., GUSCHINA, N.A., SAMOYLOV, A.V., TSAREV, Yu.N.,"The method of the effective potential for many-electron quasimolecules. Ne^{q+}- Ne (q = 1, 2, 4) collisions." Preprint of Ioffe Physical-Technical Institute N 811, Leningrad, 1983.

[5] NIKULIN, V.K., SAMOYLOV, A.V., Phys. Lett. **89A** (1982) 235.

[6] NIKULIN, V.K., GUSCHINA, N.A., Optics and spectroscopy **80** (1996) 378 (translated from Russian).

[7] BATES, D.R., McCARROLL, R., Proc. Roy. Soc. A **245** (1958) 175.

[8] HATTON, G.J., LANE, N.F., WINTER, T.G., J. Phys. B: Atom. Mol. Phys. **12** (1979) L571.

[9] NIKULIN, V.K., GUSCHINA, N.A., Atom. Plasma-Mater. Interact. Data Fusion **10** (2002) 95.

[10] NIKULIN, V.K., GUSCHINA, N.A., "Theoretical study of electron capture and excitation processes in collisions between the hydrogen-like He^+ and C^{5+}, N^{6+} ions". Preprint of Ioffe Physical-Technical Institute N 1764, St. Petersburg, 2003.

[11] NIKULIN, V.K., GUSCHINA, N.A., TSAREV, Yu.N., "Theoretical study of electron capture and excitation processes in collisions between He^+ and B^{4+}, C^{5+}, N^{6+}, O^{7+} hydrogen-like ions". Preprint of Ioffe Physical-Technical Institute N 1772, St. Petersburg, 2004.

[12] GUSCHINA, N.A., NIKULIN, V.K., "The program package for inelastic process computation in slow ion-atom collisions". Preprint of Ioffe Physical-Technical Institute N 1717, St. Petersburg, 1998.

[13] PIACENTINI, R.D., SALIN, A., Comput. Phys. Commun. **12** (1976) 199.